Discovery and quantification of lipoamino acids in bacteria

Amandine Hueber, Camille Petitfils, Pauline Le Faouder, Geoffrey Langevin, Alexandre Guy, Jean-Marie Galano, Thierry Durand, Jean-François Martin, Jean-Claude Tabet, Nicolas Cenac, et al.

Discovery and quantification of lipoamino acids in bacteria

Amandine Hueber [a, b, c], Camille Petitfils [c], Pauline Le Faouder [a, b], Geoffrey Langevin [d], Alexandre Guy [d], Jean-Marie Galano [d], Thierry Durand [d], Jean-François Martin [a, e], Jean-Claude Tabet [a, f, g], Nicolas Cenac [c, 1], Justine Bertrand-Michel [a, b, 1, *]

[a] *MetaboHUB-MetaToul, National Infrastructure of Metabolomics and Fluxomics, Toulouse, France*
[b] *I2MC, Université de Toulouse, Inserm, Université Toulouse 3 Paul Sabatier, Toulouse, France*
[c] *IRSD, Université de Toulouse, INSERM, INRA, INPENVT, Université de Toulouse 3 Paul Sabatier, Toulouse, France*
[d] *Institut des Biomolécules Max Mousseron IBMM, UMR 5247 CNRS, Université de Montpellier-ENSCM, Montpellier, France*
[e] *Toxalim (Research Centre in Food Toxicology), INRAE UMR 1331, ENVT, INP-Purpan, Paul Sabatier University (UPS), Toulouse, France*
[f] *Université Paris-Saclay, CEA, INRAE, Département Médicaments et Technologies pour la Santé (DMTS), MetaboHUB, F-91191, Gif sur Yvette, France*
[g] *Sorbonne Université, Faculté des Sciences et de l'Ingénierie, Institut Parisien de Chimie Moléculaire (IPCM), F-75005, Paris, France*

A B S T R A C T

Improving knowledge about metabolites produced by the microbiota is a key point to understand its role in human health and disease. Among them, lipoamino acid (LpAA) containing asparagine and their derivatives are bacterial metabolites which could have an impact on the host. In this study, our aim was to extend the characterization of this family. We developed a semi-targeted workflow to identify and quantify new candidates. First, the sample preparation and analytical conditions using liquid chromatography (LC) coupled to high resolution mass spectrometry (HRMS) were optimized. Using a theoretical homemade database, HRMS raw data were manually queried. This strategy allowed us to find 25 new LpAA conjugated to Asn, Gln, Asp, Glu, His, Leu, Ile, Lys, Phe, Trp and Val amino acids. These metabolites were then fully characterized by MS^2, and compared to the pure synthesized standards to validate annotation. Finally, a quantitative method was developed by LC coupled to a triple quadrupole instrument, and linearity and limit of quantification were determined. 14 new LpAA were quantified in gram positive bacteria, *Lactobacilus animalis*, and 12 LpAA in *Escherichia coli* strain Nissle 1917.

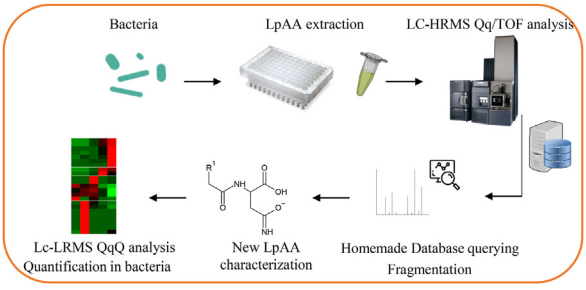

Keywords:
Lipoaminoacids
Mass spectrometry
Suspect screening
Lipidomic
Microbiota

Abbreviations: RT, retention time.

* Corresponding author. MetaboHUB-MetaToul, National Infrastructure of Metabolomics and Fluxomics, Toulouse, France.
E-mail address: justine.bertrand-michel@inserm.fr (J. Bertrand-Michel).

[1] Nicolas Cénac and Justine Bertrand-Michel jointly supervised this work.

Abbreviations

ACN	acetonitrile
AcOEt	ethyl acetate
CE	collision energy
DCM	dichloromethane
ESI	electrospray
FA	formic acid FWMH: full width at half maximum
HBTU	N,N,N′,N'-tetramethyl-O-(1H-benzotriazol-1-yl) uronium hexafluorophosphate
Hept	heptane
HLB	hydrophobic lipophilic balanced
HOBT	1-hydroxybenzotriazole
IS	internal standard
LC-HRMS	liquid chromatography high resolution mass spectrometry
LC-LRM	liquid chromatography low resolution mass spectrometry
LOD	limit of detection
LLE	liquid liquid extraction
LLOQ	lower limit of quantification
LOD	limit of detection
LOQ	limit of quantification
MeOH	methanol
MS	mass spectrometry
NMM	N-methylmorpholine
PIS	product ion scan
Qq/TOF	Quadrupole coupled to time of flight
QqQ	triple quadrupole
RF	radiofrequency
RT	retention time
SPE	solid phase extraction
SRM	selected reaction monitoring
TFA	Trifluoroacid
TIPS	triisopropyl silane
TOF	time of flight
TRIS	2-Amino-2-hydroxymethyl-propane-1,3-diol

1. Introduction

A functional microbiota is formed by the repertoire of expressed genes and, even more importantly, by proteins and metabolites. For human microbiota, a lot of studies investigated the compositional level but few studies have investigated active genes, proteins, or metabolites [1]. However, studies of molecules produced by the microbiota may be more relevant than composition when it comes to understand the role played by microbiota in host function. In fact, the taxonomic composition of the human microbiome varies tremendously across individuals, while its functional capacity is highly conserved in a same individual [2]. This conserved functional capacity is defined as the functional redundancy of the microbiota [2]. Although this redundancy is important to maintain the stability and resilience of the human microbiome, it introduces the idea that, until a certain point, species are substitutable in a given microbiota in terms of function [3]. The general aim of our consortium is to identify new metabolites produced by the gut microbiota to determine their effect on the host. In several pathologies related to intestinal microbiota dysbiosis, no increase in bacterial translocation is observed in patients indicating that, if the bacteria have an impact on the host, it is through molecules, secreted and/or transformed by the bacteria, able to cross the intestinal barrier. Amongst bacterial metabolites, several lipids including lipopeptides [4], long chain [5] and short chain fatty acid [6] or secondary bile acids [7], have been described for their capacity to cross the epithelial barrier. As in the brain, lipoamino acids (LpAA) composed by long chain unsaturated fatty acids conjugated to amino acid (AA) [8] have been identified and that we characterized lipopeptides and LpAA containing asparagine produced by *Escherichia coli* Nisle 1917 (EcN) [4], we decided to extend the discovery of LpAA from bacteria to other AA than asparagine.

In this study, a specific workflow is developed to identify and characterize new LpAAs in different bacterial strains using Liquid Chromatography High Resolution Mass Spectrometry (LC-HRMS). Advances in high-resolution mass spectrometry and tandem mass spectrometry, such as linear trap quadrupole (LTQ)/Orbitrap or hybrid Quadrupole Time-Of-Flight (Qq/TOF) technologies, offer an opportunity to rapidly screen biological and environmental specimens for a large array of chemicals using untargeted method [9–11]. To apply these global approaches, metabolites need to be present in a sufficient quantity to be characterized or at least detected, which is not our case since the concentration of our lipids of interest is quite low (about 50–70 pg.mg^{-1} of protein). Therefore, it is essential to develop a semi-targeted or suspect screening method dedicated to LpAAs. The typical approach applied in this case is a large scale suspect screening to generate semi-quantitative data in order to prioritize targeted developments. “Suspects” are defined as known compounds (“known/unknowns”) in terms of chemical name and structure which are expected (“suspected”) to be present in a sample. These approaches are often used in environmental and toxicological studies [12–15]. Even if data are acquired by HRMS, suspect screening differs from untargeted analysis because the analytes are compared to a user-defined chemical database or existing chemical inventories with manual or software-matching algorithms using accurate mass and isotope patterns. In this semi-targeted approach sample preparation plays a key role, and it needs to be adapted to the metabolites of interest [16]. In lipidomic, the two main methods which could be combined are: a liquid-liquid extraction [17] and a solid phase extraction after protein precipitation in a mixture of water and organic solvent [8,18,19].

To characterize bacterial LpAA, the different steps of the workflow developed in this project were to: 1) optimize an adapted and miniaturized chromatographic separation, 2) develop a specific sample preparation for LpAA, 3) construct a theoritical LpAA homemade database, 4) efficiently query HRMS data to find candidates and 5) characterize and confirm the new LpAA. Finally, we assessed our quantitative methods of LpAA in gram negative and positive bacteria and decipher the synthesis of this new LpAA in EcN.

2. Material and methods

2.1. Chemical and reagents

Heptane, ethyl acetate (AcOEt), methanol (MeOH), Hank's balanced salt solution (HBSS), Trizma® hydrochloride, dichloromethane (DCM), N,N,N′,N'-Tetramethyl-O-(1H-benzotriazol-1-yl) uronium hexafluorophosphate, 1-Hydroxybenzotriazole (HOBT), N-Methylmorpholine (NMM), TriFluoroAcid (TFA), triisopropyl

silane (TIPS), piperidine and C12Arg were purchased from Sigma Aldrich (Saint Quentin Fallavier, France). Acetonitrile (ACN, HRMS grade), and formic acid (HRMS grade) were purchased from Thermo Scientific. Water used in this study was purified on a milliQ system (Millipore). The 96 well-plate for solid extraction (SPE) (Oasis HLB 30 mg) were purchased from Waters (Saint-Quentin en Yvelines, France).

2.2. Standards

2.2.1. Synthesis of lipoaminolipids and lipopeptides

LpAA were synthesized following the standard procedure described in literature, by either liquid phase synthesis (LPS) or solid phase synthesis (SPS) with 2-chlorotrityl resin. In short, for LPS, the appropriate terbutyl aminoester and fatty acid were coupled with HBTU/HOBt/NMM in DCM, followed by hydrolysis of ester (and deprotection of an eventual trityl primary amide) with DCM/TFA. Purification of LpAA was carried out by Reversed Flash Chromatography (C4 or C18 column) with H_2O/MeOH or H_2O/ACN + 0.1% TFA. For SPS, appropriate Fmoc-amino acid was immobilized to 2-chlorotrityl resin with NMM in DCM. Fluorenylmethoxycarbonyl (Fmoc) protection was removed with piperidine/DCM (2/8), and resulting amine was coupled to appropriate fatty acid with HBTU/HOBt/NMM. After intensive washing, resin was cleaved with TFA/TIPS/Water (95/2.5/2.5) to obtain desired LpAA with variable yield and high purity, mostly without further purifications. Detailed synthesis of LpAA is developed in supplementary data. Internal standard (IS) used in this experiment was (S)-4-(4-amino-4-oxo-2-palmitamidobutanamido)butanoic acid substituted with 16 atoms of ^{13}C on the fatty acid chain (for detailed standard synthesis see Supplementary Information 1).

2.2.2. Standard preparation to determine linearity and reproducibility

Standard solutions were prepared in MeOH at the following concentrations 0.004, 0.19, 0.07, 0.30, 1.22, 4.88, 19.53, 78.13, 312.5 and 1250 pg.μL^{-1} for all primary standards. The concentration of the IS *C16AsnGABA was 600 pg μL^{-1}. Calibration curves were calculated by the ratio between the analyte area and the internal standard area.

2.3. Bacterial samples

2.3.1. EcN bacteria strains and culture conditions

Escherichia coli strain Nissle 1917 (EcN) (serotype O6:K5:H1), the isogenic mutants EcNΔclbA, EcNΔclbN and EcNΔclbP were used in this study. Gene inactivation was engineered using the lambda red recombinase method [20] and deletions were confirmed by using flanking primers. EcNwt, EcNΔclbA, EcNΔclbN, and EcNΔclbP were grown on LB agar plates supplemented with kanamycin (50 $\mu g\ mL^{-1}$) when required. After overnight incubation at 37 °C, single colonies of each strain were seeded in 3 mL of LB with antibiotics (when needed) and incubated overnight at 37 °C in agitation (250 rpm). Bacteria were then inoculated at OD600 = 0.05 in 10 mL of minimal medium A (K_2HPO_4 10.5 g.L^{-1}; KH_2PO_4 4.5 g.L^{-1}; $(NH_4)_2SO_4$ 1 g.L^{-1}; sodium citrate 0.5 g.L^{-1}; $MgSO_4$ 0.2 g.L^{-1}, thiamine 0,1 g.L^{-1}, and glucose 3%) supplemented with kanamycin (when required) and cultures were grown for 12 h at 37 °C under shaking conditions (250 rpm). The last step was repeated one more time by inoculating the bacteria at OD600 = 0.02 for 24 h before sampling them. The bacteria were stored at -80 °C before the LpAA and lipopeptide extraction.

2.3.2. Anaerobic bacteria strain and culture conditions

Lactobacillus animalis (DSMZ strain n°20602) was grown on Lactobacilli MRS broth (Difco, Fisher scientific SAS, Illkirch, France) − agar plates supplemented with cysteine chloride monohydrate 0.5 g.L^{-1}. After 24 h of incubation at 37 °C, 3 colonies were seeded in 30 mL of MRS broth supplemented with cysteine chloride monohydrate 0.5 g.L^{-1} (Merck − Sigma Aldrich, St. Quentin Fallavier, France) and incubated overnight at 37 °C. All the culture steps have been performed in a hypoxic environment ensured by using a Whitley H35 hypoxystation (don Whitley scientific, Bingley, United Kingdom) and all the incubations were done in an anaeropack jar (Fisher scientific SAS, Illkirch, France) with an anaeroGen sachet (Fisher scientific SAS, Illkirch, France) to ensure an anaerobic environment.

2.4. Sample preparation

2.4.1. Extraction of LpAA and lipopeptides

For the extraction, 500 µL of Tris buffer (pH = 9), 1 mL of MeOH and 10 µL of IS *C16AsnGABA were added to the bacterial pellets and crushed with a Fast Prep instrument (MP Biomedicals), using two cycles (6,5 m s^{-1}, 30 s). Ten µL of suspension were withdrawn for protein quantification with Biorad assays, then, 6.6 mL of water were added to the homogenate. Samples were centrifuged at 1016×*g* for 15 min (4 °C) and the supernatants submitted to SPE using HLB plates (Oasis HLB, 30 mg, Waters). Plates were conditioned with 750 µL ethyl acetate, 750 µL MeOH and 750 µL H_2O:MeOH (90:10; v/v). Samples were loaded at a flow rate of one drop per 2 s and SPE plates washed using 1 mL H_2O:MeOH (90:10; v/v) followed by 1 mL heptane. Lipopeptides were eluted using 1 mL AcN, 1 mL MeOH and 1 mL AcOEt. Eluent were carefully removed from the plate, and transferred to a Pyrex tube, dried under nitrogen gas and reconstituted in 10 µL MeOH for LC-HRMS analysis. Extract was stored at −20 °C before LC-MS analysis.

2.4.2. Validation of the LpAA specific sample preparation

The extraction yield and the matrix effect were determined to validate the preparation of bacteria. Briefly, three sets of bacteria (*ECN*) were prepared according to section 2.4.1 in triplicate: 1) bacteria were extracted without IS; 2) bacteria were extracted without IS and IS were spiked in the final extract at three different concentrations (1000 pg μL^{-1}, 500 pg.μL^{-1} and 250 pg.μL^{-1}) and 3) bacteria were spiked with the three different concentrations of IS and then extracted. The extraction yield was determined as the difference between peak areas of IS in pre-spiked (condition 3) and post-spiked samples (condition 2). Condition 1 was used to ensure the absence of IS in bacteria. The matrix effect was determined as the difference between peak areas of IS added to the extracted samples (condition 2) and pure IS. Two independent experiments have been performed.

2.5. High resolution mass spectrometry analysis

2.5.1. LC-MS/MS conditions

The acquity UPLC-I-Class system (Waters) was equipped with CSH C18 column Waters (1 × 100 mm; 2,7 µm), as analytical column, and maintained at 40 °C. The mobile phases consisted of H_2O:HCO_2H (99.9:0.1; v/v) (A) and ACN:HCO_2H (99.9:0.1, v/v) (B). Flow rate was 0.15 mL min^{-1}. The multi-step gradient was as follow: 25% B at 0 min, 100% B at 16 min, 100% B at 18 min, 25% B at 18,1 until 20 min (Condition A). The autosampler (Acquity UPLC-I-Class FTN) was set at 4 °C, and the injection volume was 1 µL per analysis. UPLC was coupled on-line to a Xevo G2-XS time of flight (Qq/TOF) (Waters, Saint-Quentin en Yvelines, France) equipped with electrospray ionization (ESI). The MS, MS^E and MS/MS analysis were achieved in positive and negative ionization mode, in 2 separate runs with a full-width at half maximum (FWHM)

resolution of 16 000 (*m/z* 400). For the MS analysis, source temperature was 120 °C, cone voltage was set at 40 kV, nebulizer gas flow rate was 400 L h^{-1} and desolvation temperature was set at 380 °C. The analysis was performed in continuum mode for both the MS and MS [2] experiments. Mass spectra were recorded in MS and MS^E modes from *m/z* 50 to *m/z* 750. For the MS [2] experiments, nitrogen was the target gas in the XS collision cell (as segmented RF only quadrupole), ion precursors were isolated at ± 5 m/z for the required sensitivity. MS [2] experiments were carried out under low energy collisional activation conditions. The collision energy (E_{LAB}) was optimized using synthesized standards to maintain the precursor ion relative abundance at 30%. The best condition was an E_{LAB} of 20 eV for LpAA and lipopeptides. For the full characterization of C13Asn, the same flow rate and solvent A and B were used, starting with 48% of A at 0 min, 60% at 40 min, and 2 min to return on initial conditions (Condition B) and the same mass spectrometer parameters were applied.

2.5.2. Data processing

Unifi software (Version 1.9.4.053): data in continuum mode were loaded to the software. For the automatic identification by Unifi, the homemade database was added to the Unifi library and then to the analysis method as expected precursor. The analysis parameters were set as follow: *find 3D peaks*: at low energy peak intensity threshold was 2500 counts and *m/z* range was set between 30 m/z and 600 *m/z*, at higher energy peak intensity threshold was 80 counts, and *m/z* range was set between 150 m/z and 600 m/z; noise level was set at high level: 100000 counts; *3D peak detection*: without any restriction of retention time; *3D isotope cluster* was set at 0.3. In addition to the protonated MH^+ or deprotonated $[M-H]^-$ molecules, the adduct $[M+Na]^+$ or $[M+HCOO]^-$ ions was chosen for each precursor molecules under positive and negative ionization modes, respectively. The allowed score was set at 8. The software has been set to automatically search expected fragments: deprotonated amino-acid (for the 20 AA), AA ammoniac loss $[AA-H)-NH_3]^-$ (noted as $(z-2H)^-$ with nomenclature showed Fig. 1), deprotonated gamma-aminobutyric acid $[GABA-H]^-$, and fatty amid from C8 alkyl chain to C19 alkyl chain (i.e $[C_{12}H_{24}NO-H]^-$ noted as Lpc^-). The software has been set to automatically search neutral loss corresponding to the GABA loss: 103,0633. The mass error accepted for the precursor ion was set at 20 ppm, and at 2 mDa for the expected fragment ions.

QuanLynx software (application from MassLynx software, Version 4.2): reprocessing method were created to query *m/z*, with 5 ppm error accepted for the deprotonated molecule from the theoritical homemade database, without any RT restriction.

2.6. Low resolution mass spectrometry analysis

2.6.1. LC-MS/MS conditions

High-performance liquid chromatography system was a Shimadzu Mikros LC system, equipped with a thermostatted autosampler SIL-30AC, a rack changer II, a Nexera Mikros binary pump, a degasser on-line DGU-20A3R and a LTO-Mikros column oven. As for HRMS analysis, the analytical column was a CSH C18 column Waters (1 × 100 mm; 2,7 µm) and was maintained at 40 °C. The mobile phases consisted of water:formic acid (99.9:0.1; v/v) (A) and acetonitrile:HCO_2H (99.9:0.1, v/v) (B). Flow rate was 0.1 mL.min^{-1}. The multi-step gradient starts with 30% B at 0 min, 80% B at 13 min, 100% B at 13.5 min, 100% B at 16 min, and at 16.5 min 30% B until 18 min. The chromatography system was coupled online to a triple quadrupole mass spectrometer Shimadzu 8060 equipped with a ESI source in negative mode and was optimized as follow: *nebulizer*: 2 L.min^{-1}; *desolvation line*: 250 °C; *heating-block*: 450 °C, *heating gaz flow*: 10 L.min^{-1}, and no drying gas was used. Argon gas (purity, >99.9995%) was used for collision-induced dissociation (CID).

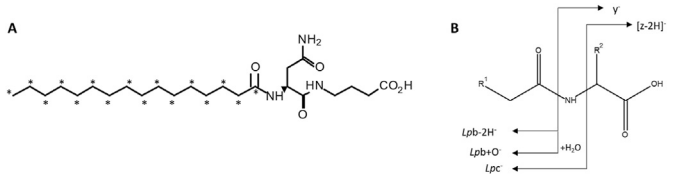

Fig. 1. (**A**) Structure of the labelled ^{13}C16:0-AsnGABA internal standard (* = ^{13}C); (**B**) nomenclature of product ions from dissociation of the deprotonated lipo-amino-acids (Hueber et al., Amino Acid, Submitted).

Identification tools: the detector was programmed to profile putative compounds using theoretical SRM transition deducted from LpAA fragmentation with variation of fatty acid length. For instance, for C12Asn (previously characterized [4], the MRM transitions were {$[M-H]^-$; $[(M-H_2O)-H]]^-$} and {$[M-H]^-$; Lpc^-} corresponding to {313; 295} and {313; 198}. So to identify the other compounds of the series, we determined the theoretical MRM transitions for various alkyl chain length, e.g. the theoretical MRM of the C13Asn were {327; 309} and {327; 212}. This method was applied to all the amino acids identified in the bacterial LpAA.

Quantification tools: for each metabolite the MRM transition was optimized on the pure standard to get the best selectivity and the best sensitivity with a qualitative and a quantitative transition and was programmed to monitor a 2 min-window (expected chromatographic retention time ± 1 min). The dwelltime were optimized for each compound and were set between 30 and 100 msec.

2.6.2. Data processing

Peak detection, integration and quantitative analysis were performed by Labsolution Post run and Insight software (Version 5.99 SP2, Shimadzu, Kyoto, Japan). Concentration of the analytes in samples were calculated by calibration curves (Section 2.2.2). LOQ (Limit of Quantification) was determined using 3 calibration ranges in triplicate. LLOQ (Lower Limit of Quantification) were determined for accuracy (coefficient of variation) and precision (CV) in the range of 80–120% and LOQ for the accuracy and precision in the range of 85–115%. Linear dynamic range was determined as the range from LOQ to the highest calibration point reached. LOD (Limit of Detection) measured in biological samples was defined as a level with a signal-to-noise ratio (S/N) of 3.

3. Results and discussion

3.1. Analytical optimization to improve LpAA detection

3.1.1. Chromatographic separation and detection

A mixture of pure metabolites was used to develop the semi-targeted analysis. We tried to choose a broad spectrum of structures with different biophysical properties such as: C12AsnGABA, C12Asn, C14Asn, C16 and C18 hydroxy fatty acids, C20:4 or C18:1 acyl serotonin and 20:4 or 18:1 acyl anandamide at a concentration of 1 ng.µL^{-1}. As an internal standard, we need a molecule close to the one studied but absent of our matrix then a labelled derivative of CxAsnGABA was chosen. First, we synthetized a C12AsnGABA with the C12:0 fully deuterated. Due to a poor quality of labelled precursor, we finally synthetized a fully ^{13}C16:0AsnGABA labelled on the fatty acid (Fig. 1). This internal standard was added to the mixture of standards to develop the analytical method.

The first step of the workflow was to optimize the chromatographic separation. The classical method used to separate free oxylipins and hydroxylated fatty acids under low resolution LC/ESI-MS/MS conditions [21,22] was adapted for the high-resolution Qq/

TOF instrument. To improve the sensitivity, the C18 2.1 mm diameter column was replaced by a 1 mm diameter columns with a reduction of flow rate from 0.4 mL.min^{-1} to 0.15 mL.min^{-1}. The total ionic current obtained for a EcN extract was increased by 87% (data not shown).

The mixture of standards was used to adjust the MS parameters in order to obtain the best sensitivity. Both the desolvation voltage and source temperature modifications did not improved the sensitivity. The gas flow was optimized between 500 and 800 L.h^{-1} to an optimal value at 800 L.h^{-1} in negative ionization mode and at 600 L.h^{-1} in positive ionization mode. The radiofrequency (RF) only quadrupole offset voltage was set with an optimum value at 130 V in both ionization modes. These optimizations allowed to achieve an average detection improvement of 15% for both the LpAA and lipopeptides compounds.

3.1.2. Sample preparation

Two main protocols are typically used to extract fatty acid metabolites: liquid-liquid extraction (LLE) and solid phase extraction (SPE). Bligh and Dyer LLE using a mixture of MeOH, $CHCl_3$ and H_2O is used in limited number of studies [23], others used heptane and ethyl acetate, instead of MeOH and $CHCl_3$ to extract endocannobinoid with efficient yield [24]. Nevertheless, the use of SPE after protein precipitation in a mixture of water and solvent (e.g. methanol, acetone or acetonitrile) is classically used in lipidomic for this family of lipids. Different types of SPE sorbent are used: polymeric reverse-phase sorbent plate for free oxylipins [21], C18 cartridge combined with ACN elution for surfactine, a bacterial lipopeptide [25], C18 sorbent combined with hexane and isopropanol elution for anandamide and N-Acyl-ethanolamine [26], or normal phase SPE to extract endocannabinoid from human tissues [27]. LLE and SPE could be combined to extract isoprostane [28] or acyl aminoacid with a series of complex SPE enrichment step [8].

Due to the ubiquity of lipids, no blank matrix is available to measure extraction yield, then a mixture of C12Asn, C14Asn, C14AsnGABA and IS at a concentration of 1 ng. µL^{-1} in solvent was used to assay the extraction. First, classic Bligh and Dyer extraction was tested. Even with addition of an acid (0.1% of acetic acid or 0.1% of HCl) to extract acidic metabolite after protonation, the extraction yield was very low and variable from one metabolite to another (data not shown). Then, two different strategies were tested: one using HLB SPE purification and another one using LLE extraction (Table S1). For SPE, standards and IS were homogenized in MeOH:H_2O (2:1; v/v) or in MeOH:TRIS pH 9 (2:1; v/v). After a centrifugation to precipitate the proteins, a dilution to 15% of methanol was performed. The metabolites were eluted by ACN, MeOH and AcOEt in a first method, by MeOH and CH_2Cl_2 in a second, or by ACN, MeOH and CH_2Cl_2 in a last one. The best yield of recovery (between 29% and 68%) for the 3 metabolites tested and for the IS were obtained with the first method (Table S1). For LLE, the best results were obtained with ethyl acetate in presence of water. However, to obtain clear extract ready to inject in case of complex matrix such as bacteria or tissue, the protocol has been completed by a washing step with heptane to remove neutral lipid [29]. This latter step induced the loss of C14Asn and IS and a lack of reproducibility. So, SPE combined with ACN, MeOH and AcOEt elution was chosen.

3.1.3. Validation of the sample preparation

To validate the sample preparation, extractions of EcN pellets (n = 3; 2 independent experiments) were performed with different concentrations of IS (250, 500 and 1000 pg µL^{-1}). In parallel, EcN pellets were extracted without internal standard which was added at the three concentrations at the end of the preparation. These different protocols compared to the non-extracted ISTD allowed the calculation of preparation yield and of the matrix effect. The preparation yield was similar between the different concentrations, with a recovery of 29.6% ± 3.3% for 1000 pg.µL^{-1}, 26.3% ± 7.2% for 500 pg.µL^{-1} and 43.6% ± 14.2% for 250 pg.µL^{-1}. The matrix effect was also similar between the different concentrations: with a recovery of 35.7% ± 1.3% for 1000 pg.µL^{-1}, 30.8% ± 3.2% for 500 pg.µL^{-1} and 26.2% ± 8% for 250 pg.µL^{-1}.

3.2. Workflow for the discovery of new LpAA

3.2.1. Theoretical lipopeptides and LpAA library inspired by C14Asn and C12AsnGABA

To query the LpAA of interest in lipid extracts, a homemade database has been constructed based on an amide linkage between a fatty acid and an amino acid or/and neurotransmitter (serotonin, dopamine, GABA or histamine). The length of fatty acid, as usually described in bacteria [30], was between 8 and 19 carbon atoms, saturated or with one unsaturation (or one cyclopropane which present the same mass default), with or without one hydroxyl group. 28 putative fatty acids were generated and one of the 20 natural amino-acids or an ornithine has been added (588 molecules) or one neurotransmitter such as GABA, serotonin, dopamine or histamine (84 molecules). Finally, each fatty acid linked to one amino acid were conjugated to one neurotransmitter (serotonin, dopamine, GABA or histamine) to propose 1764 molecules. These different associations generated at the end 2436 possible structures. For each putative metabolite, structural drawing, elemental composition of the $[M\text{-}H]^-$ and $[M+H]^+$ molecular species with the corresponding accurate *m/z* values have been generated and added to Unifi or QuanLynx Waters tools (Database not shown).

3.2.2. Acquisition of the data to provide putative candidate by spectral analogy

The lipid extracts were injected on the LC-Qq/TOF mass spectrometer to acquire data in MS^E continuum and centroid recording, in both positive and negative ionization modes. The continuum scan is required for the sample reprocessing with Unifi software, but not for Quanlynx software. The analysis on continuum mode generated heavy data (8 Giga octet per analyzed sample), compared to the centroid one (1 Giga octet per analyzed sample), which is not suitable to analyze large series of sample under large throughput conditions. First, we used the Unifi software to increase probability to find new LpAA or lipopeptides using the research of the neurotransmitter's common neutral losses or the expected fragment ions by analogy to the fragmentations describes for the C12Asn, C14Asn and C12AsnGABA [31] assuming that the same fragmentation pathways can occur under low energy collision conditions for the LpAA homologues. Nevertheless, after several tests on bacterial samples, this application was unable to find candidates. Candidates were only identified in a concentrated standards mixture (1 ng µL^{-1}). Even when a match occurred in the database, Unifi proposed a structure for the MS/MS associated fragment ions with an erroneous interpretation. In our hands, identification of new compounds using this software function worked only for metabolites present at a higher concentration than our metabolites of interest. If the intensity threshold was enhanced at the maximum to identify a maximum of compounds, more than 50 000 matches, impossible to check manually, were generated. In contrast, if this threshold was not enhanced at the maximum, some LpAA were not identified. In addition, when several compounds characterized by different molecular masses co-eluate, their respective molecular ionic species were activated together and their respective product ions were recorded together. Consequently, for each precursor ion, the software attributes the same product ions without distinction of their origin. Sometimes, for one fragment ion of interest, the

software indicated more than 50 precursors ions that should be checked manually. Finally, we concluded that the Unifi software was unsuitable for the identification of LpAA in complex mixtures.

Finally, we used QuanLynx (an application from MassLynx software, Waters usually applied to quantify metabolites) to automatically query our candidates in the homemade database where the precursor ions as deprotonated $[M-H]^-$ molecules were added regardless of retention time. For each automatic match, which could be the natural isotopic peak or an isobaric isotopomer, we had to check manually the presence of the natural isotopic cluster for each putative candidate in order to confirm that the match was the deprotonated molecule. Even if it was time consuming, the use of QuanLynx seems to be the best option for our purpose. This workflow has been used to identify LpAA in lipid extracted from *EcN* and *L. animalis*. We obtained 162 potential matches from the 2436 available compounds in the database, and after the isotopologue verification, 25 of them were real matches that needed to be fully characterized.

3.2.3. Characterization of the structure of a new LpAA: C13-Asn

The putative identification of C13-Asn by MassLynx was first done by attribution of its monoisotopic molecular mass (Mw = 328.2317 Da) from the mixture separation in μLC-HRMS and molecular deprotonation of compounds under negative ESI conditions. MS/MS analyses suggest the proposed LpAA structure *via* its gas phase fragmentations (through simple cleavages or rearrangements) of the deprotonated [LpAA-H] molecule.

3.2.3.1. Improvement of the chromatographic separation of C13-Asn. Using the chromatographic separation "conditions **A**", the analyzed selected ions were a broad peak cluster (ranging from *m/z* 326 to *m/z* 330, Fig. 2(a), **(b)**). Even if the peaks between *m/z* 328 and *m/z* 330 were the most intense signals persisting at higher E_{lab} values, it was possible to detect peaks at the *m/z* 327 nominal values as expected for the [C13Asn-H] ion (window of Fig. 2(a)). In addition to the peak at *m/z* 327.2274 (i.e., the [C13Asn-H] ion of interest), few isobaric ions, less intense than the neighboring satellite peaks ranging from *m/z* 328 and *m/z* 330, appeared between *m/z* 326.9867 and *m/z* 327.9867. Consequently, the product ion spectrum exhibited a lot of unexpected peaks impossible to interpret on the base of the [LpAA-H] ion structure. Indeed, recorded at E_{lab} = 5 eV, the product ion spectrum displays only few fragment ions at *m/z* 311.2354 (15.9920 Da loss), *m/z* 295.2689 (31.9587 Da loss) and *m/z* 190.8965 (136.3309 Da loss) which were inconsistent with dissociations of the putative [C13Asn-H] ion at *m/z* 327.2274. These losses cannot be attributed to fragmentations of the expected [C13Asn-H] ion (*m/z* 327.2274) but rather, either to its isobaric ions (at *m/z* 327.2682, *m/z* 327.1608, and *m/z* 326.9867) or to the other selected ions at the *m/z* 328-m/z 330 scale. At higher collision energy (Fig. 2(b)), the previous unknown signals were maintained except *m/z* 190 which was shifted at *m/z* 183.0229. Furthermore, additional peaks at *m/z* 255.2102 and *m/z* 269.2231 appear in addition to the expected peaks at *m/z* 309, *m/z* 265, *m/z* 238, *m/z* 212, *m/z* 131, *m/z* 114 and *m/z* 96 (Table S2). The results obtained at higher collision energy confirmed that fragmentations take place from either the isobaric ion mixture or/and higher mass precursor ions together, according to different relative stabilities under low energy collision conditions.

By improvement of chromatographic conditions (conditions B), peaks at the *m/z* 327 nominal values (at 5 eV Fig. 2(c)) were almost exclusively constituted by the [C13Asn-H] ion (*m/z* 327.2274). The CID spectrum exhibited very weak intense peaks at *m/z* 311 and *m/z* 285 which were not expected. This suggested that the precursor ions related to the isobaric compounds which co-elutes with C13Asn, were more fragile toward the CID processes. The peaks at *m/z* 311 and *m/z* 285 disappear at E_{lab} = 20 eV (Fig. 2(d)) and then, the product ion spectrum was characterized by the exclusive presence of the expected fragment ions of [C13Asn-H] with less than 5 ppm of error (Table S2). However, a main signal arises at *m/z* 327.1645 in addition to the peak at *m/z* 327.2274 ion (window in Fig. 2(d)). The intensity of the peak at *m/z* 327.2274 was strongly decreased at the high collision energy compared to the low collision energy (window in Fig. 2(c)) while the intensity of its satellite peak at *m/z* 327.1645 was very low at low energy. This suggests that the *m/z* 327.2274 ion was significantly less stable than its isobaric ion at *m/z* 327.1645 with an unknown structure.

Interestingly, at low collision energy (5 eV, Fig. 2(e)), the CID spectrum of *m/z* 327 of the synthetic C13Asn did not display fragmentation which was not the case for the CID spectrum of the natural product under same collision conditions (Fig. 2(a)). This confirmed the fragility of unknown isobaric ions relative to [C13Asn-H] and its satellite peaks of the *m/z* 328 - *m/z* 330 zone. Finally, both the product ion spectra (Fig. 2(d) and (f)) of *m/z* 327 provided from biological mixture and from synthetic sample were stackable as two identical fingerprints. The structure proposed to the *m/z* 327.2274 ion was confirmed and the different product ions of its CID spectrum were completely rationalized on the basis of the [C13Asn-H] structure.

3.2.3.2. Main displayed fragmentations in product ion spectra of the deprotonated C13-Asn. General interpretations of even-electron molecular ionic species are based on the following considerations: (i) deprotonation can occur competitively at carboxylic acid, amide and enolizable ester sites resulting in a mixture of various [LpAA-H] deprotomers [32], (ii) the negative (or positive) charge exclusively promotes fragmentations under low collision energy conditions and (iii) dissociations may yield simple cleavages as well as rearrangements. The latter can occur directly or through stepwise processes (e.g. *via* isomerization into ion-dipole intermediates prior to complete dissociation) [33]. Due to the role of the charge, different competitive bond cleavages can take place according to the charge location.

The CID spectrum rationalization can allow the selection of the most relevant collision energy to reach the best sensitivity for the elucidation of the LpAA molecule structure and the best specificity for its quantification. To illustrate this purpose, we detailed the dissociations of the [C13Asn-H] ion (*m/z* 327) activated under the E_{Lab} = 20 eV conditions.

Favored loss of water from [C13Asn-H]. This abundant loss yielding *m/z* 309 was particularly specific and was observed independently to the length of fatty acid moiety (its relative abundance is larger than 50%). Indeed, its signal appeared as the base peak (at E_{Lab} = 20 eV, Fig. 2(f)) in the CID spectrum. It reached an optimum of 56.8% intensity relative to the total ionic current (TIC) at E_{Lab} = 20 eV as shown in the energy resolved mass spectrometry (ERMS) breakdown curves (Fig. S1). Such water release did not exceed an optimum of 10% of TIC (Table S2) for the most abundant one as demonstrated from ERMS of the other studied deprotonated [LpAA-H] species (ERMS not reported). Thus, the water loss must be assisted by the functional group of the AA side chain since this loss is totally hinder from LpAA with non-polar AA moiety. Consequently, the amide group must be deprotonated to drive a nucleophilic attack at the carboxyl site yielding *via* cyclization, a tetrahedral intermediate (Scheme 1(a)). This one isomerized by C–OH bond cleavage into an OH ion/[(C13Asn-H)-OH] neutral complex from which OH removed one proton to the neutral and the resulting complex dissociated by water release and formation of [(C13Asn-H)-H_2O] (*m/z* 309). This carboxylate derivate carries a nitrile leaving group capable of being subsequently released.

Consecutive losses of (H_2O + CO_2) and (H_2O + CO_2+HCN) yielding

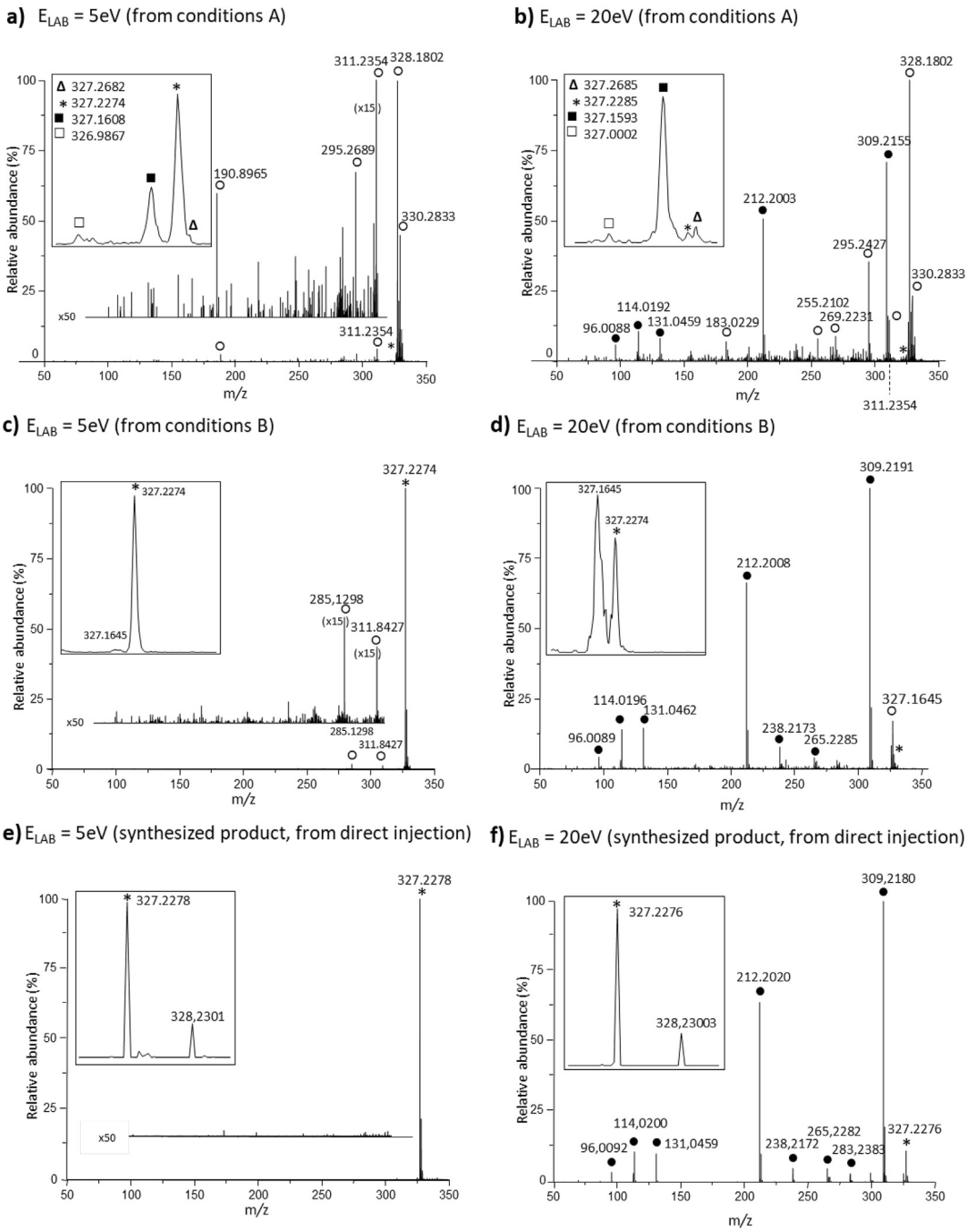

Fig. 2. Product ion spectra of *m/z* 327 generated from μLC-HRMS in negative ESI mode under the A separative conditions (a)–(b) and under the B conditions (c)–(d) from biological sample, and by direct injection from synthetic C13Asn sample (e)–(f) under low energy collision conditions: (a)-(c)-(e) E_{Lab} = 5 eV and (b)-(d)-(f) at E_{Lab} = 20 eV. Normalized *m/z* molecular zone in window of each product ion spectrum and in (a) and (b) the peak intensities of the *m/z* 100-m/z 310 scale were amplified by a factor of 50). In product ion spectra (b) and (d), the used annotations of peaks (with intensity >5% of base peak) are (i) the asterisk (*) for expected precursor ion, (ii) the empty circle (○) for unexpected peaks and (iii) the full circle (●) for expected peaks attributed to [C13Asn-H] (according to Table S2 in Supplementary Information).

m/z 265 and m/z 238. The CO_2 loss consecutive to that of H_2O was assisted by a 1–4 proton transfer from the amide enolizable α position to the carbon atom which initially carried the CO_2 lost to obtain the [(C13Asn-H)-H_2O-CO_2] enolate (*m/z* 265, Scheme 1(b)). Consecutively, the alkoxy site can assist the loss of the leaving CN group through internal nucleophilic substitution. By this way, the CN ion/[(C13Asn-H)-(H_2O + CO_2+CN] neutral complex was formed, and internal proton transfer from enamine site to CN allowed the elimination of HCN and led to formation of *m/z* 238 as a deprotonated 2-alkyl-oxazoline form (Scheme 1(b)).

Competitive formation of complementary m/z 212 and m/z 114 ion pair. From the deprotomer molecular species (originated from the water loss, with the charge at the enolizable position of the amide group of Asn), the moiety side chain migrated concomitantly with proton from the neighbored carboxylic acid group. This step led to the RCONH-CH bond cleavage yielding ion/dipole complex

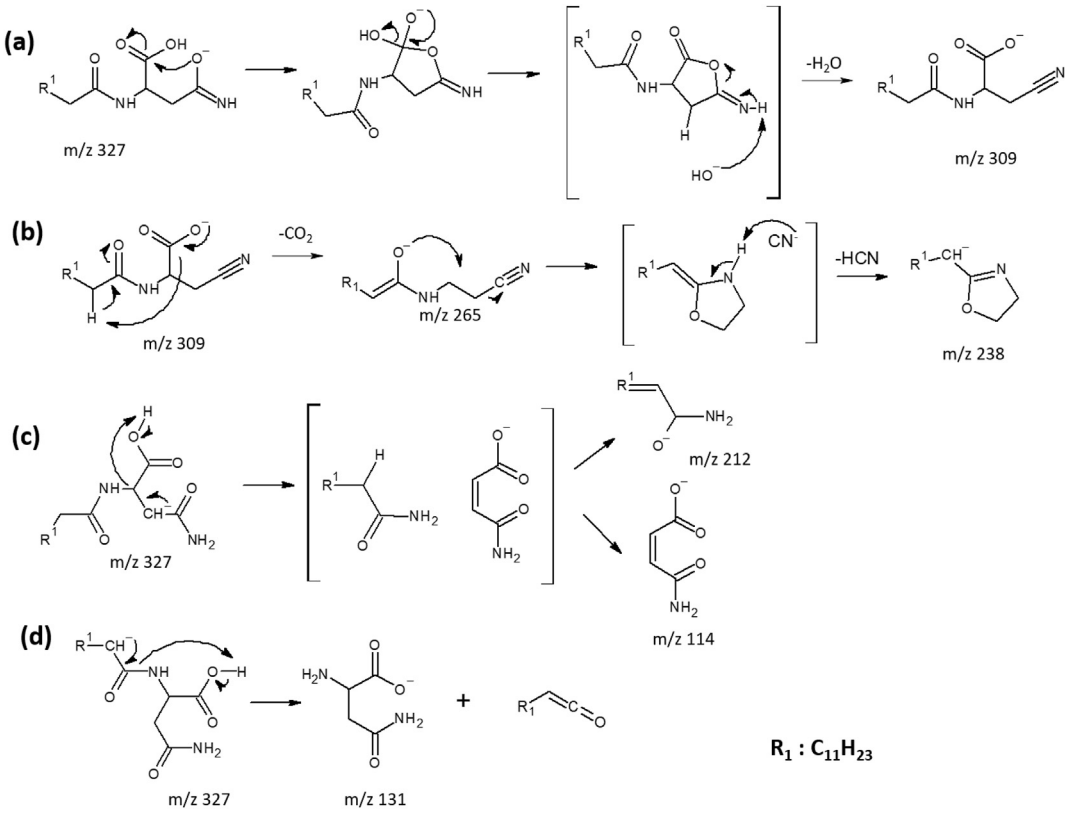

Scheme 1. Proposed formation of major product anions from the LpAA C13Asn (*m/z* 327) product anion.

constituted by deprotonated maleic acid monoamide and fatty acid amide. This complex can directly dissociated to release the fatty acid amide leading to formation of *m/z* 114 (ion $[z\text{-}2H]^-$) or after an inter-partner proton transfer, the isomerized complex can decomposed into fatty acid amidate (ion *Lpc*$^-$, *m/z* 212) (Scheme 1(c)).

Formation of deprotonated asparagine (m/z 131). The CO—NH bond cleavage was promoted by the neighbored negative charge at the enolizable position of the amide linkage combined with proton migration from carboxylic group to nitrogen site. By this pathway, the fatty acid ketene was directly released (Scheme 1(d)) and was not enough acid to form an ion/dipole by molecular species isomerization prior to dissociation.

After C13Asn full fragment pattern elucidation, the same identification has been expanded to other LpAA found by suspect screening experiments performed on a LC-LRMS/MS using triple quadrupole instrument more sensitive than the Qq/TOF tandem. From previous MS [2] characterization, it could be possible to predict theoretical MS/MS according to the alkyl chain length and to the deprotonated amino acid as product anions. These MRM transitions were programmed on μLC-QqQ method to analyze bacterial extracts. Due to the improved sensitivity, this approach permitted to find 54 putative new LpAA: C14:1Asn, C15Asn, C16Asn, C16:1Asn, C17Asn, C17:1Asn, C12:1Leu/Ile, C13Leu/Ile, C14Leu/Ile, C14:1Leu/Ile, C15Leu/Ile, C15:1Leu/Ile, C16Leu/Ile, C16:1Leu/Ile, C17Leu/Ile, C17:1Leu/Ile, C18Leu/Ile, C18:1Leu/Ile, C12Gln, C12:1Gln, C13Val, C14Val, C14:1Val, C15Val, C16Val, C16:1Val, C17:1Val, C18Val, C12Glu, C12:1Glu, C16Glu, C15:1Glu, C16Glu, C17:1Glu, C12Lys, C12:1Lys, C14Lys, C15Lys, C16Lys, C16:1Lys, C17Lys, C17:1Lys, C12:1Phe, C13Phe, C14Phe, C14:1Phe, C15Phe, C15:1Phe, C16Phe, C16:1Phe, C17Phe, C17:1Phe, C18Phe and C18:1Phe. These compounds were identified in LC-LRMS, without a level 1 of identification which correspond to metabolites fully characterized and identified. Two orthogonal analysis methods of an authentic chemical standard analyzed in the same laboratory is mandatory for this level of identification. In addition, the standard should be compared to experimentally identified metabolite in the same laboratory with the same analytical method [34]. These 54 compounds were identified with a level 3 of identification corresponding to metabolites with incomplete or putative annotation. However, this method didn't allow the identification of LpAA with serine, ornithine, methionine, alanine, cysteine and threonine.

We decided to characterize the most abundant LpAA and at least one per family. We focused on the whole LpAsn family (C12:1Asn, C14:1Asn, C15Asn, C16:1Asn, C17Asn, C17:1Asn), and on C12Lys, C14Lys, C12Glu, C14Glu, C16Glu, C12Asp, C12Gln, C12Val, C12Trp, C12Arg, C12His, C12Leu, C12Ile, and C14Phe. These compounds were synthetized (except C12Arginine which were purchased from Sigma Aldrich) to be fully characterized by MS [2], with an identification level 1 or level 2, to permit construction of the quantitative method (Table S2).

3.2.3.3. Full characterization of 22 new bacterial LpAA. Following the principle of elucidation detailed for the C13Asn, 22 LpAA were fully characterized with their fragmentation pattern (Table S2). These 22 molecules were composed by a fatty acid (from C12 to C17) conjugated to one of 12 following amino acid: asparagine, arginine, aspartate, glutamine, glutamate, histidine, leucine/isoleucine, lysine, phenylalanine, tryptophan and valine. The dissociations presented in section 3.2.3.2 (Scheme 1) were similar for all the LpAsn (except the product ions containing the fatty acid moiety) to those displayed in the product ion spectra of the deprotonated C12Asn, C12:1Asn, C14Asn, C14:1Asn, C15Asn, C16Asn, C17Asn and C17:1Asn molecules.

The consecutive losses of (H_2O + CO_2) and (H_2O + CO_2+HCN) presented in section 3.2.3.2 (Scheme 1 (b)) yielding *m/z* 265 and *m/z* 238 for the C13Asn, were specific to the LpAsn family (Lp being C12:1, C12, C13, C14:1, C14, C15, C16:1, C16, C17:1 and C17) and to LpGln and LpHis even if the abundance of these ions were low (Table S2). The loss of water of the [C12Gln-H]$^-$ (*m/z* 327) was strongly reduced to 4% compared to the 56.8% observed for [C13Asn-H] (*m/z* 327). Such a difference has been already described for the dissociation of the free [Asp-H] and [Glu-H] anion. Concerning the observed (H_2O + CO_2+HCN) loss sequence of the [C12His-H] ion (*m/z* 336), the previous proposed mechanisms cannot be involved. The water loss was possible, due to the large gas phase acidity of the imidazole group of the histidine moiety and induced a bicyclic system from which, the consecutive losses of CO_2 and (CO_2+HCN) were produced by dissociation pathways as reported in Scheme S1.

The formation of the fatty acid amidate (ion *Lpc*$^-$, Fig. 1(b)) and its complementary [z-2H] ion specifically occurred from LpAA with amide group on the side chain of amino-acid moiety (Asn and Gln) *via* a similar mechanism (Scheme 1(c)). Note that in competition with this ion pair, formation of deprotonated amino acid (i.e., y$^-$) took place favorably from [LpGln-H]. When this amide group was exchanged by a carboxyl group (i.e., Asp and Glu), only the fatty acid amidate, *Lpc*$^-$, was detected with an intensity of 38% of TIC for [LpAsp-H] and 4% at maximum for [LpGlu-H]. However, the abundance reduction of *Lpc*$^-$, [z-2H] and y$^-$ (or their disappearance) was accompanied by a strong emergence of fatty acid carboxylate (i.e., [*Lp*b + O]) and deprotonated amino-acid anhydride (i.e., [*y*-H_2O]) as a complementary product ion pair. This regeneration of deprotonated fatty acid was specific to the [LpAsp-H] and [LpGlu-H] precursor ions. For LpAA conjugates with basic AA moieties (i.e., Lys, Arg and His), with aromatic side chain (Phe and Trp) and with non-polar amino acids (Val, Leu and Ile), these above competitive ion pairs were replaced by deprotonated amino-acid (y) with abundance higher than 30% (except for Arg). The y abundance was re-enforced (>50% of TIC) mainly from non-polar side chain AA.

To conclude, the 22 LpAA discovered in this study were characterized by MS [2], but to reach the level 1 of identification, it was necessary to compare the candidates to the pure synthesized compounds which allow to verify the fragmentation pattern and the retention time.

Table 1
Comparison of discovered aminolipids measured in bacterial sample and pure synthetized compounds: retention time (RT) comparison with RSD% calculation, *m/z* with error ppm.

		RT LC-HRMS (min)	% RSD	RT LC-LRMS (min)	% RSD	Elementary composition	*m/z* calculated [M − H]$^-$	*m/z* experimental (HRMS)	Erreur (ppm)
C12-ASN	Synthesized	3.72	0,56	5.89	0,36	$C_{16}H_{30}N_2O_4$	313.2132	313.2119	4.4
	Sample	3.75		5.86				313.2120	4.1
C12:1-ASN	Synthesized	5.70	0,12	4.81	0,14	$C_{16}H_{28}N_2O_4$	311.1976	311.1972	1.4
	Sample	5.69		4.80				311.1980	1.2
C13-ASN	Synthesized	5.42	1,16	7.04	0,40	$C_{17}H_{32}N_2O_4$	327.2289	327.2274	4.7
	Sample	5.51		7.00				327.2274	4.7
C14-ASN	Synthesized	6.60	0,63	8.18	0	$C_{18}H_{34}N_2O_4$	341.2445	341.2443	0.8
	Sample	6.66		8.18				341.2446	0.1
C14:1-ASN	Synthesized	7.68	0,27	6.79	0	$C_{18}H_{32}N_2O_4$	339.2289	339.2278	3.3
	Sample	7.65		6.79				339.2296	2.0
C15-ASN	Synthesized	8.69	0,24	9.34	0,07	$C_{19}H_{36}N_2O_4$	355.2602	355.2599	0.9
	Sample	8.66		9.33				355.2605	0.8
C16-ASN	Synthesized	7.27	0,88	10.51	0	$C_{20}H_{38}N_2O_4$	369.2758	369.2752	1.8
	Sample	7.18		10.51				369.2769	2.8
C16:1-ASN	Synthesized	9.66	0,14	8.91	0	$C_{20}H_{36}N_2O_4$	367.2602	367.2600	2.1
	Sample	9.64		8.91				367.2602	0.1
C17-ASN	Synthesized	8.14	0,77	11.67	0,06	$C_{21}H_{40}N_2O_4$	383.2915	383.2914	0.3
	Sample	8.23		11.68				383.2914	0.3
C17:1-ASN	Synthesized	8.18	0,25	9.99	0	$C_{21}H_{38}N_2O_4$	381.2758	381.2758	0.1
	Sample	8.15		9.99				381.2752	1.8
C12-ARG	Synthetized	2.30	0,61	3.09	0,45	$C_{18}H_{36}N_4O_3$	355.2714	355.2714	0.1
	Sample	2.32		3.07				355.2714	0.1
C12-ASP	Synthesized	5.48	0,25	6.83	0	$C_{16}H_{29}NO_5$	314.1972	314.1974	0.1
	Sample	5.46		6.83				314.1941	10.2
C12-GLN	Synthetized	4.63	0,30	5.86	0,36	$C_{17}H_{32}N_2O_4$	327.2289	327.2288	0.4
	Sample	4.61		5.83				327.2277	3.8
C12-GLU	Synthesized	5.42	0,39	6.84	0,10	$C_{17}H_{30}NO_5$	328.2129	328.2122	2.2
	Sample	5.45		6.83				328.2136	2.0
C14-GLU	Synthesized	7.36	0,28	9.10	0	$C_{19}H_{34}NO_5$	356.2422	356.2427	4.3
	Sample	7.39		9.10				356.2420	6.3
C16-GLU	Synthesized	9.33	0,07	11.37	0; 06	$C_{21}H_{38}NO_5$	384.2755	384.2756	0.2
	Sample	9.32		11.38				384.2755	0.1
C12−HIS	Synthesized	2.19	1,59	2.96	0,47	$C_{18}H_{31}N_3O_3$	336.2292	336.2290	0.8
	Sample	2.24		2.94				336.2303	3.1
C12-LYS	Synthesized	2.12	0,99	2.89	0,49	$C_{18}H_{36}N_2O_3$	327.2653	327.2646	0.3
	Sample	2.15		2.87				327.2653	0.1
C14-LYS	Synthesized	3.57	0,98	4.57	0,76	$C_{20}H_{40}N_2O_3$	355.2966	355.2961	1.4
	Sample	3.62		4.62				355.2959	2.0
C12-LEU/ LEU	Synthesized	8.73	0,24	8.68	0,16	$C_{18}H_{35}NO_3$	312.2544	312.2540	1.3
	Sample	8.76		8.66				312.2542	0.7
C14-PHE	Synthesized	10.84	0,32	13.00	0,05	$C_{23}H_{37}NO_3$	374.2700	374.2699	0.4
	Sample	10.79		12.99				374.2700	0.1
C12-TRP	Synthesized	8.26	0,51	10.04	0	$C_{23}H_{34}N_2O_3$	385.2496	385.2496	0.1
	Sample	8.20		10.04				385.2497	0.1
C12-VAL	Synthetized	7.95	0	9.81	0	$C_{17}H_{33}NO_3$	298.2387	298.2379	2.9
	Sample	7.95		9.81				298.2387	0.1

3.2.4. Validation for the discovered structures

So pure synthesized standards were analyzed in the same conditions than bacterial extracts, and HRMS analyses permitted to confirm *m/z* ratios and retention time (Table 1). Herein, even with the use of standards, the double bond or hydroxyl positions on fatty acid moiety could not be determined. The level of annotation for each LpAA characterized is indicated in Table 1.

Even if LpAA composed by Phe and Val associated to C20:4, C22:6 or C18:1 fatty acid have been described in brain [8], from the 2200 theoretical aminolipids database, we identified 10 new LpAA in EcN (*Escherichia coli* strain Nissle 1917): C13Asn, C14:1Asn, C15Asn, C16Asn, C16:1Asn, C17:1Asn, C12Glu, C12Lys, C12His and C12Asp; and 15 LpAA in *Lactobacillus animalis*: C12Arg, C14Glu, C12Lys, C14Lys, C12His, C12Gln, C12Asp, C14:1Asn, C16:1Asn, C15Asn, C12Trp, C12Val, C12Leu/Ile, C16Asn and C14Phe.

3.3. Quantification of new aminolipid in bacteria

3.3.1. Development of a sensitive method by LC-MS/MS

To study these new aminolipid in bacteria or in complex matrixes such as intestines or stools it is essential to develop a robust sensitive and quantitative method. As we gave priority to sensitivity in front of resolution, we developed this method on a LR-MS triple quadrupole detection Shimadzu 8060 system coupled to a μLC. In order to achieve the necessary selectivity and sensitivity of the method, the source parameter and the mass detection were optimized. For the source parameters nebulizer was assayed from 1 to 5 L min^{-1}; desolvation line from 150 to 250 °C; interface temperature from 100 to 300 °C; heating-block from 300 to 450 °C, heating gas flow from 0 to 10 L min^{-1}, and finally dry gas at 0 L min^{-1} in order to obtain the best compromise. Analyses were performed in Selected Reaction Monitoring (SRM) detection mode using argon as a collision gas. Optimization for each compounds were done automatically with LabSolution software. The quantification transition chosen for each compound was the more abundant, even if it was not a specific transition. The 2 transitions used for qualitative analysis were chosen among the most abundant with exclusion of the quantitative transition. The values of Q1 pre bias, energy collision and Q3 pre bias were automatically optimized by the software. For example for the C13Asn metabolite, the quantitative transition was {*m/z* 327}/{*m/z* 309} corresponding to the $[M - H]^-/[(M - H_2O)-H^-]$ and the two qualitative transitions were {*m/z* 327}/{*m/z* 212} corresponding to the $[M - H]^-/[(RCONH_2)-H^-]$ and {*m/z* 327}/{*m/z* 131} corresponding to the $[M - H]^-/[(\text{Amino acid})-H^-]$. The same transition (qualitative and quantitative) scheme was effective for all the LpAA in this study, and are report in Table 2 (the second qualitative transition is not shown). Collision energy were optimized to obtain the best detection for each standard (Table 2).

3.3.2. Sensitivity, linearity and reproducibility of the method

To study the sensitivity and the linearity of the quantitative method, calibration lines with 10 calibration points from 0.004 to 1250 pg μl^{-1} (with 600 pg μL^{-1} of IS) were analyzed 3 times in triplicates. The limit of detection (LOD) used in the analytical method of biological samples was defined as the level with a signal-to-noise ratio (S/N) of 3. The limit of quantification (LOQ) was determined by measuring the level with a signal-to-noise ratio (S/N) greater than 10 and with an accuracy and precision within the range of 80–120%. The accuracy and the precision of all 10 calibration points above LOQ were in the range of 85–115%. The Linear dynamic range was determined as the range from LOQ to the highest calibration point corresponding to the conditions described above (Table 2). Repeatability and precision were respectively calculated using relative standard deviation (% RSD) and accuracy for all range of concentrations of pure standards in triplicates, they were under 2% (data not shown). The same experiment was done to assay the inter-day variations, calibration curves were analyzed twice, with 15 days between analyses, and RSD were under 5%. The method allowed the quantification of LpAA with a great sensitivity with a LOQ between 0.39 and 1.56 pg injected, and a large linearity range from LOD until 1250 pg injected.

3.3.3. LpAA quantification in EcN and L. animalis

Our quantitative method has been used to study LpAA synthesis by a gram negative bacteria EcN and a gram positive Lactobacillus

Table 2
SRM characterization with quantitative and qualitative transition, energy applied to generate the transition (EC et Q1/Q3PreBias), Linear regression equation and correlation R2.

Compound	Linear regression	R^2	LOD ($pg.\mu L^{-1}$)	LOQ ($pg.\mu L^{-1}$)	Quantitative MRM transition	Q1 Pre Bias (V)	EC (eV)	Q3 Pre Bias (V)	Qualitative MRM transition
C12:1Asn	y = 49290x - 173866	0.9990	0.39	1.56	312 → 293	30	15	13	311 → 183
C13Asn	y = 63564x - 222566	0.9984	0.19	1.56	327 → 309	34	18	15	327 → 212
C14:1Asn	y = 132014x - 110079	0.9977	0.19	0.78	339 → 321	14	17	22	339 → 224
C15Asn	y = 25510x - 65143	0.9996	0.39	1.56	355 → 240	25	24	16	355 → 337
C16Asn	y = 64907x - 151246	0.9990	0.19	0.39	369 → 351	15	20	16	369 → 254
C16:1Asn	y = 53376x - 199389	0.9995	0.78	1.56	367 → 349	28	20	26	367 → 252
C17Asn	y = 137315x - 20177	0.9978	0.39	0.78	383 → 365	15	20	18	383 → 96
C17:1Asn	y = 40608x - 117983	0.9989	0.19	0.78	381 → 363	14	25	10	381 → 266
C12Arg	y = 15767x - 105656	0.9988	0.04	0.78	355 → 131	20	26	20	355 → 131
C12Asp	y = 44937x - 317123	0.9950	0.19	0.78	314 → 198	24	23	21	314 → 199
C12Gln	y = 22434x - 40015	0.9985	0.19	0.39	327 → 198	24	28	23	327 → 127
C12Glu	y = 27518x - 86993	0.9991	0.19	1.56	328 → 198	10	20	20	328 → 128
C14Glu	y = 49107x - 214246	0.9983	0.19	0.78	356 → 226	26	22	24	356 → 128
C16Glu	y = 1262x - 19015	0.9943	0.19	0.78	384 → 255	30	23	8	384 → 128
C12His	y = 30227x - 77911	0.9987	0.39	0.78	336 → 110	25	27	10	336 → 154
C12Leu	y = 181029x - 418227	0.9990	0.04	1.56	313 → 130	13	29	26	312 → 268
C12Ile	y = 236326x - 425633	0.9985	0.04	1.56	313 → 130	12	29	26	312 → 268
C12Lys	y = 45468x - 202933	0.9976	0.19	1.56	327 → 145	13	25	27	327 → 283
C14Lys	y = 70865x - 401950	0.9988	0.19	0.78	355 → 145	14	25	27	355 → 311
C14Phe	y = 81754x - 29953	0.9981	0.19	0.78	374 → 164	15	24	29	374 → 226
C12Pro	y = 77314x - 52780	0.9975	0.19	1.56	296 → 114	21	21	11	296 → 198
C12Trp	y = 46967x - 173680	0.9987	0.19	1.56	385 → 203	14	21	20	285 → 256
C12Val	y = 180951x - 433184	0.9988	0.04	0.39	298 → 116	22	22	12	298 → 254

animalis. In wild-type EcN, we quantified the C12Asn, C13Asn, C14Asn, C14:1Asn, C15Asn, C16Asn, C16:1Asn, C17:1Asn, C12Glu, C12Asp, C12AsnBABA and C12AsnGABA, and in Lactobacillus animalis the C12Lys, C14Lys, C12His, C12Gln, C12Asp, C14:1Asn, C16:1Asn, C15Asn, C17Asn, C12Trp, C12Val, C12Leu, C16Asn and C14Phe (Fig. 3, Table S3).

EcN is known to harbour a genomic island, named pks, which carries a cluster of genes that enables the synthesis of LpAA and of a genotoxin called colibactin [35–38]. This toxin is produced by a complex biosynthetic machinery involving the sequential action of proteins ClbA to ClbS [39]. ClbA, a phosphopantetheinyl transferase (PPTase) essential for the activation of the NRPS and PKS enzymes [39], is mandatory for the biosynthesis of colibactin [35] but is also involved in the biosynthesis of other bioactive metabolites such as the siderophores enterobactin, salmochelin and yersiniabactin [40]. Following activation by ClbA, the initiating NRPS ClbN uses Asn as a substrate to generate an N-myristoyl-D-Asn (C14Asn). The NRPS-PKS assembly line continues the synthesis of precolibactin compound(s) using malonyl-coA and different amino acids [36–38] as substrates. The precolibactin is then cleaved by peptidase ClbP to liberate colibactin and N-myristoyl-D-Asn [36–38].

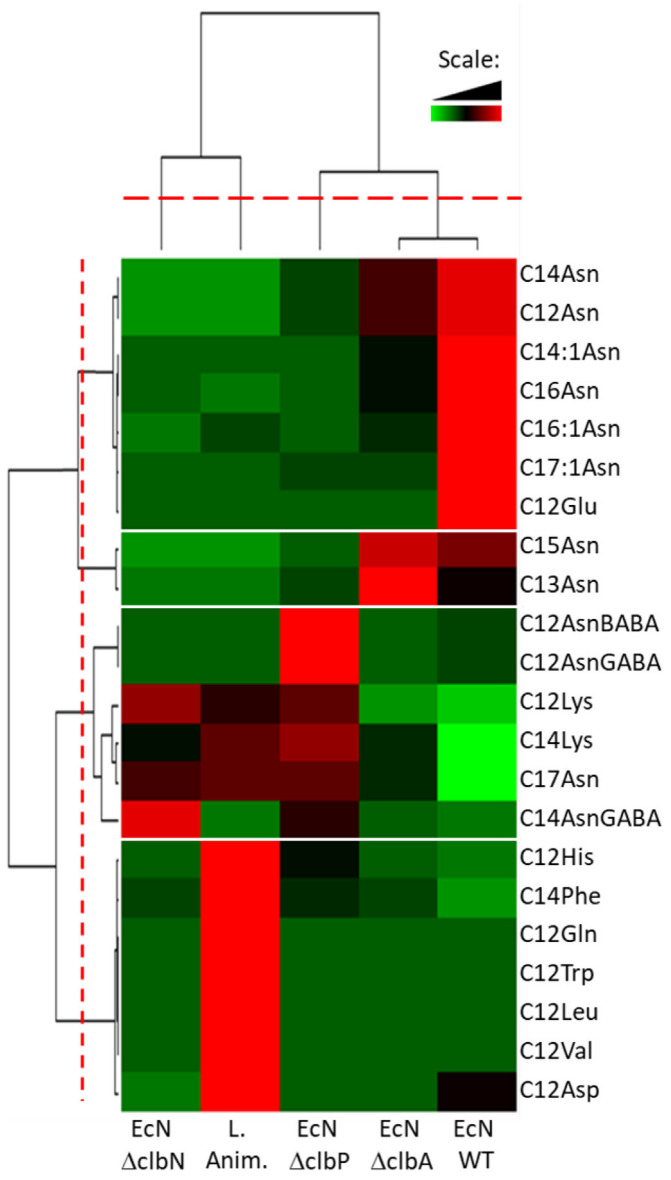

Fig. 3. Heat map of LpAA and Lipoeptides quantified by LC-MS/MS. Data are shown in a matrix format: Each row represents a single lipid, and each column represents a bacterial strain: Escherichia coli strain Nissle 1917 wild type (EcN WT) or delated for specific gene of the pks island (clbN, clbA or clbP) and Lactobacillus animalis (L. Anim.). Each color patch represents the normalized quantity of lipid (row) in a bacterial strain (column), with a continuum of quantity from bright green (lowest) to bright red (highest). The pattern and length of the branches in the left dendrogram reflect the relatedness of the lipids and in the top dendogram, the realatedness of the bacterial strains. The dashed red lines are the dendrogram distance used to cluster lipids or bacteria. (For interpretation of the references to color in this figure legend, the reader is referred to the Web version of this article.)

In order to determine the implication of ClbA, ClbN and ClbP in the synthesis of the different identified lipids, LpAA were quantified in EcN wild type, in EcN deleted for ClbA, ClbN or ClbP, and in L. animalis. Hierarchical clustering of LpAA amounts quantified in bacterial pellets (pg/mg of proteins) was used to reveal the main differences between them (Fig. 3). LpAA formed 4 different clusters. The first cluster was constituted by LpAA with a concentration decreased in EcN ΔclbA, ΔclbP and ΔclbN compared to EcN WT and not expressed in L. animalis. The synthesis of these LpAA was dependent on clbA, clbN and clbP as previously described for the C14asn. The second cluster discriminated LpAA which need clbN and clbP but not clbA to be produce and not present in L. animalis. The third cluster was composed by LpAA expressed in EcN deleted for ClbN and ClbP, and in L. animalis. Finally, the fourth cluster was composed by LpAA expressed mainly in L. animalis. All together these data indicated that these gram negative and gram positive bacteria produced LpAA. In addition, a single deletion of genes modified not only the concentration but also the nature of LpAA demonstrating the importance to quantify a large panel of LpAA when studying bacterial metabolites.

4. Conclusion

In conclusion, we developed a workflow which potentially allows the identification of the 2436 compounds of our database using mass spectrometry. The structural determination of the compounds by mass spectrometry and its validation with pure synthetized standards are two important steps for the characterization of LpAA and lipopeptides as their low concentration do not allowed their analysis either by NMR or/and by X-ray, which would require more than several tens of μg and several mg, respectively. This method allowed the characterization and quantification of 22 new LpAA in bacteria. Our quantitative method could be applied to more complex matrix such as patient feces or biopsies in order to determine the role of these bacterial molecules in diseases related to microbiota dysbiosis. This method represents a unique opportunity to connect an innovative and quantitative method to clinical applications to investigate LpAA synthesis by patient microbiota.

Funding resources

This work was supported by the French National Institutes of Health (Inserm) and Region Occitanie. NC is a recipient of the grant from ANR (ANR-18-CE14-0039-01) and NC & JBM are recipient of the grant from ANR (ANR-20-CE14-0011-01).

CRediT authorship contribution statement

Amandine Hueber: Conceptualization, Data curation, Visualization, Investigation, Writing – original draft, Writing – review & editing. **Camille Petitfils:** Resources. **Pauline Le Faouder:** Resources, Conceptualization. **Geoffrey Langevin:** Organic Synthesis. **Alexandre Guy:** Organic Synthesis. **Jean-Marie Galano:** Organic Synthesis. **Thierry Durand:** Organic Synthesis. **Jean-François Martin:** Visualization, Investigation. **Jean-Claude Tabet:** Writing –

original draft, Writing – review & editing. **Nicolas Cenac:** Writing – original draft, Writing – review & editing, Supervision, Conceptualization, Project administration, Funding acquisition. **Justine Bertrand-Michel:** Conceptualization, Writing – original draft, Writing – review & editing, Supervision, Conceptualization, Project administration, Funding acquisition.

Declaration of competing interest

The authors declare that they have no known competing financial interests or personal relationships that could have appeared to influence the work reported in this paper.

Acknowledgements

Mass spectrometry analysis were done on MetaToul (Toulouse metabolomics & fluxomics facilities, www.metatoul.fr) which is part of the French National Infrastructure for Metabolomics and Fluxomics MetaboHUB-ANR-11-INBS-0010. We would like to thank Hanna Kulyk-Barbier for helpful discussions.

Appendix A. Supplementary data

Supplementary data to this article can be found online at https://doi.org/10.1016/j.aca.2021.339316.

References

[1] P. Lepage, M.C. Leclerc, M. Joossens, S. Mondot, H.M. Blottière, J. Raes, D. Ehrlich, J. Doré, A metagenomic Insight into our gut's microbiome, Gut 62 (1) (2013) 146–158, https://doi.org/10.1136/gutjnl-2011-301805.

[2] S.D. Allison, J.B.H. Martiny, Resistance, resilience, and redundancy in microbial communities, Proc. Natl. Acad. Sci. Unit. States Am. 105 (Supplement 1) (2008) 11512–11519, https://doi.org/10.1073/pnas.0801925105.

[3] A.E. Pérez-Cobas, A. Artacho, H. Knecht, M.L. Ferrús, A. Friedrichs, S.J. Ott, A. Moya, A. Latorre, M.J. Gosalbes, Differential effects of antibiotic therapy on the structure and function of human gut microbiota, PLoS One 8 (11) (2013), e80201, https://doi.org/10.1371/journal.pone.0080201.

[4] T. Pérez-Berezo, J. Pujo, P. Martin, P. Le Faouder, J.-M. Galano, A. Guy, C. Knauf, J.C. Tabet, S. Tronnet, F. Barreau, M. Heuillet, G. Dietrich, J. Bertrand-Michel, T. Durand, E. Oswald, N. Cenac, Identification of an analgesic lipopeptide produced by the probiotic Escherichia coli strain Nissle 1917, Nat. Commun. 8 (1) (2017) 1314, https://doi.org/10.1038/s41467-017-01403-9.

[5] J. Pujo, C. Petitfils, P. Le Faouder, V. Eeckhaut, G. Payros, S. Maurel, T. Perez-Berezo, M. Van Hul, F. Barreau, C. Blanpied, S. Chavanas, F. Van Immerseel, J. Bertrand-Michel, E. Oswald, C. Knauf, G. Dietrich, P.D. Cani, N. Cenac, Bacteria-derived long chain fatty acid exhibits anti-inflammatory properties in colitis, Gut 70 (6) (2021) 1088–1097, https://doi.org/10.1136/gutjnl-2020-321173.

[6] E. Pouteau, I. Meirim, S. Métairon, L.-B. Fay, Acetate, propionate and butyrate in plasma: determination of the concentration and isotopic enrichment by gas chromatography/mass spectrometry with positive chemical ionization: SCFA concentration and isotopic enrichment in plasma, J. Mass Spectrom. 36 (7) (2001) 798–805, https://doi.org/10.1002/jms.181.

[7] R. Berkecz, F. Tömösi, T. Körmöczi, V. Szegedi, J. Horváth, T. Janáky, Comprehensive phospholipid and sphingomyelin profiling of different brain regions in mouse model of anxiety disorder using online two-dimensional (HILIC/RP)-LC/MS method, J. Pharmaceut. Biomed. Anal. 149 (2018) 308–317, https://doi.org/10.1016/j.jpba.2017.10.043.

[8] B. Tan, D.K. O'Dell, Y.W. Yu, M.F. Monn, H.V. Hughes, S. Burstein, J.M. Walker, Identification of endogenous acyl amino acids based on a targeted lipidomics approach, J. Lipid Res. 51 (1) (2010) 112–119, https://doi.org/10.1194/jlr.M900198-JLR200.

[9] S.S. Andra, C. Austin, D. Patel, G. Dolios, M. Awawda, M. Arora, Trends in the application of high-resolution mass spectrometry for human biomonitoring: an analytical primer to studying the environmental chemical space of the human exposome, Environ. Int. 100 (2017) 32–61, https://doi.org/10.1016/j.envint.2016.11.026.

[10] E.L. Schymanski, J. Jeon, R. Gulde, K. Fenner, M. Ruff, H.P. Singer, J. Hollender, Identifying small molecules via high resolution mass spectrometry: communicating confidence, Environ. Sci. Technol. 48 (4) (2014) 2097–2098, https://doi.org/10.1021/es5002105.

[11] E.L. Schymanski, H.P. Singer, J. Slobodnik, I.M. Ipolyi, P. Oswald, M. Krauss, T. Schulze, P. Haglund, T. Letzel, S. Grosse, N.S. Thomaidis, A. Bletsou, C. Zwiener, M. Ibáñez, T. Portolés, R. de Boer, M.J. Reid, M. Onghena, U. Kunkel, W. Schulz, A. Guillon, N. Noyon, G. Leroy, P. Bados, S. Bogialli, D. Stipaničev, P. Rostkowski, J. Hollender, Non-target screening with high-resolution mass spectrometry: critical review using a collaborative trial on water analysis, Anal. Bioanal. Chem. 407 (21) (2015) 6237–6255, https://doi.org/10.1007/s00216-015-8681-7.

[12] M.G.E. Guardian, P. He, A. Bermudez, S. Duan, S.S. Kaushal, E. Rosenfeldt, D.S. Aga, Optimized suspect screening approach for a comprehensive assessment of the impact of best management practices in reducing micropollutants transport in the potomac river watershed, Water Res. X 11 (2021) 100088, https://doi.org/10.1016/j.wroa.2021.100088.

[13] A. Wang, R.R. Gerona, J.M. Schwartz, T. Lin, M. Sirota, R. Morello-Frosch, T.J. Woodruff, A suspect screening method for characterizing multiple chemical exposures among a demographically diverse population of pregnant women in San Francisco, Environ. Health Perspect. 126 (7) (2018), 077009, https://doi.org/10.1289/EHP2920.

[14] J.M. Colby, K.L. Thoren, K.L. Lynch, Suspect screening using LC–QqTOF is a useful tool for detecting drugs in biological samples, J. Anal. Toxicol. 42 (4) (2018) 207–213, https://doi.org/10.1093/jat/bkx107.

[15] M. Pourchet, L. Debrauwer, J. Klanova, E.J. Price, A. Covaci, N. Caballero-Casero, H. Oberacher, M. Lamoree, A. Damont, F. Fenaille, J. Vlaanderen, J. Meijer, M. Krauss, D. Sarigiannis, R. Barouki, B. Le Bizec, J.-P. Antignac, Suspect and non-targeted screening of chemicals of emerging concern for human biomonitoring, environmental health studies and support to risk assessment: from promises to challenges and harmonisation issues, Environ. Int. 139 (2020) 105545, https://doi.org/10.1016/j.envint.2020.105545.

[16] I. Liakh, T. Sledzinski, L. Kaska, P. Mozolewska, A. Mika, Sample preparation methods for lipidomics approaches used in studies of obesity, Molecules 25 (22) (2020) 5307, https://doi.org/10.3390/molecules25225307.

[17] P. Manirakiza, A. Covaci, P. Schepens, Comparative study on total lipid determination using soxhlet, roese-gottlieb, Bligh & dyer, and modified Bligh & dyer extraction methods, J. Food Compos. Anal. 14 (1) (2001) 93–100, https://doi.org/10.1006/jfca.2000.0972.

[18] C.C. Teo, W.P.K. Chong, E. Tan, N.B. Basri, Z.J. Low, Y.S. Ho, Advances in sample preparation and analytical techniques for lipidomics study of clinical samples, TrAC Trends Anal. Chem. (Reference Ed.) 66 (2015) 1–18, https://doi.org/10.1016/j.trac.2014.10.010.

[19] A. Dupuy, P. Le Faouder, C. Vigor, C. Oger, J.-M. Galano, C. Dray, J.C.-Y. Lee, P. Valet, C. Gladine, T. Durand, J. Bertrand-Michel, Simultaneous quantitative profiling of 20 isoprostanoids from omega-3 and omega-6 polyunsaturated fatty acids by LC–MS/MS in various biological samples, Anal. Chim. Acta 921 (2016) 46–58, https://doi.org/10.1016/j.aca.2016.03.024.

[20] K.A. Datsenko, B.L. Wanner, One-step inactivation of chromosomal genes in Escherichia coli K-12 using PCR products, Proc. Natl. Acad. Sci. Unit. States Am. 97 (12) (2000) 6640–6645, https://doi.org/10.1073/pnas.120163297.

[21] P. Le Faouder, V. Baillif, I. Spreadbury, J.-P. Motta, P. Rousset, G. Chêne, C. Guigné, F. Tercé, S. Vanner, N. Vergnolle, J. Bertrand-Michel, M. Dubourdeau, N. Cenac, LC–MS/MS method for rapid and concomitant quantification of pro-inflammatory and pro-resolving polyunsaturated fatty acid metabolites, J. Chromatogr. B 932 (2013) 123–133, https://doi.org/10.1016/j.jchromb.2013.06.014.

[22] J. Pujo, C. Petitfils, P. Le Faouder, V. Eeckhaut, G. Payros, S. Maurel, T. Perez-Berezo, M. Van Hul, F. Barreau, C. Blanpied, S. Chavanas, F. Van Immerseel, J. Bertrand-Michel, E. Oswald, C. Knauf, G. Dietrich, P.D. Cani, N. Cenac, Bacteria-derived long chain fatty acid exhibits anti-inflammatory properties in colitis, Gut 70 (6) (2021) 1088–1097, https://doi.org/10.1136/gutjnl-2020-321173.

[23] E.G. Bligh, W.J. Dyer, A rapid method of total lipid extraction and purification, Can. J. Biochem. Physiol. 37 (8) (1959) 911–917, https://doi.org/10.1139/o59-099.

[24] A.A. Zoerner, S. Batkai, M.-T. Suchy, F.-M. Gutzki, S. Engeli, J. Jordan, D. Tsikas, Simultaneous UPLC–MS/MS quantification of the endocannabinoids 2-arachidonoyl glycerol (2AG), 1-arachidonoyl glycerol (1AG), and anandamide in human plasma: minimization of matrix-effects, 2AG/1AG isomerization and degradation by toluene solvent extraction, J. Chromatogr. B 883–884 (2012) 161–171, https://doi.org/10.1016/j.jchromb.2011.06.025.

[25] M. Alajlani, A. Shiekh, S. Hasnain, A. Brantner, Purification of bioactive lipopeptides produced by Bacillus subtilis strain BIA, Chromatographia 79 (21–22) (2016) 1527–1532, https://doi.org/10.1007/s10337-016-3164-3.

[26] C. Garst, M. Fulmer, D. Thewke, S. Brown, Optimized extraction of 2-arachidonyl glycerol and anandamide from aortic tissue and plasma for quantification by LC-MS/MS: endocannabinoid extraction from tissue and plasma, Eur. J. Lipid Sci. Technol. 118 (5) (2016) 814–820, https://doi.org/10.1002/ejlt.201500115.

[27] V. Mutemberezi, J. Masquelier, O. Guillemot-Legris, G.G. Muccioli, Development and validation of an HPLC-MS method for the simultaneous quantification of key oxysterols, endocannabinoids, and ceramides: variations in metabolic syndrome, Anal. Bioanal. Chem. 408 (3) (2016) 733–745, https://doi.org/10.1007/s00216-015-9150-z.

[28] A. Dupuy, P. Le Faouder, C. Vigor, C. Oger, J.-M. Galano, C. Dray, J.C.-Y. Lee, P. Valet, C. Gladine, T. Durand, J. Bertrand-Michel, Simultaneous quantitative profiling of 20 isoprostanoids from omega-3 and omega-6 polyunsaturated fatty acids by LC–MS/MS in various biological samples, Anal. Chim. Acta 921 (2016) 46–58, https://doi.org/10.1016/j.aca.2016.03.024.

[29] J. Dalli, R.A. Colas, M.E. Walker, C.N. Serhan, Lipid mediator metabolomics via LC-MS/MS profiling and analysis, in: M. Giera (Ed.), Clinical Metabolomics, Methods in Molecular Biology, vol. 1730, Springer New York, New York, NY,

2018, pp. 59–72, https://doi.org/10.1007/978-1-4939-7592-1_4.
[30] H. Goldfine, Bacterial membranes and lipid packing theory, J. Lipid Res. 25 (13) (1984) 1501–1507, https://doi.org/10.1016/S0022-2275(20)34423-0.
[31] J. Pujo, C. Petitfils, P. Le Faouder, V. Eeckhaut, G. Payros, S. Maurel, T. Perez-Berezo, M. Van Hul, F. Barreau, C. Blanpied, S. Chavanas, F. Van Immerseel, J. Bertrand-Michel, E. Oswald, C. Knauf, G. Dietrich, P.D. Cani, N. Cenac, Bacteria-derived long chain fatty acid exhibits anti-inflammatory properties in colitis, Gut 70 (6) (2021) 1088–1097, https://doi.org/10.1136/gutjnl-2020-321173.
[32] E. Darii, Y. Gimbert, S. Alves, A. Damont, A. Perret, A.S. Woods, F. Fenaille, J.-C. Tabet, First direct evidence of interpartner hydride/deuteride exchanges for stored sodiated arginine/fructose-6-phosphate complex anions within salt-solvated structures, J. Am. Soc. Mass Spectrom. 32 (6) (2021) 1424–1440, https://doi.org/10.1021/jasms.1c00040.
[33] R.B. Cole (Ed.), Electrospray and MALDI Mass Spectrometry: Fundamentals, Instrumentation, Practicalities, and Biological Applications, second ed., Wiley, Hoboken, N.J, 2010.
[34] R.M. Salek, C. Steinbeck, M.R. Viant, R. Goodacre, W.B. Dunn, The role of reporting standards for metabolite annotation and identification in metabolomic studies, GigaScience 2 (1) (2013) 13, https://doi.org/10.1186/2047-217X-2-13.
[35] J.-P. Nougayrede, Escherichia coli induces DNA double-strand breaks in eukaryotic cells, Science 313 (5788) (2006) 848–851, https://doi.org/10.1126/science.1127059.
[36] X. Bian, J. Fu, A. Plaza, J. Herrmann, D. Pistorius, A.F. Stewart, Y. Zhang, R. Müller, In vivo evidence for a prodrug activation mechanism during colibactin maturation, Chembiochem 14 (10) (2013) 1194–1197, https://doi.org/10.1002/cbic.201300208.
[37] C.A. Brotherton, E.P. Balskus, A prodrug resistance mechanism is involved in colibactin biosynthesis and cytotoxicity, J. Am. Chem. Soc. 135 (9) (2013) 3359–3362, https://doi.org/10.1021/ja312154m.
[38] M.I. Vizcaino, P. Engel, E. Trautman, J.M. Crawford, Comparative metabolomics and structural characterizations illuminate colibactin pathway-dependent small molecules, J. Am. Chem. Soc. 136 (26) (2014) 9244–9247, https://doi.org/10.1021/ja503450q.
[39] F. Taieb, C. Petit, J.-P. Nougayrède, E. Oswald, The enterobacterial genotoxins: cytolethal distending toxin and colibactin, EcoSal Plus 7 (1) (2016), https://doi.org/10.1128/ecosalplus.ESP-0008-2016 ecosalplus.ESP-0008-2016.
[40] P. Martin, I. Marcq, G. Magistro, M. Penary, C. Garcie, D. Payros, M. Boury, M. Olier, J.-P. Nougayrède, M. Audebert, C. Chalut, S. Schubert, E. Oswald, Interplay between siderophores and colibactin genotoxin biosynthetic pathways in Escherichia coli, PLoS Pathog. 9 (7) (2013), e1003437, https://doi.org/10.1371/journal.ppat.1003437.